Polymer Chemistry

Structural Insight into the Viscoelastic Behaviour of Elastomeric Polyesters: Effect of the Nature of Fatty Acid Side Chains and Degree of Unsaturation

Journal:	*Polymer Chemistry*
Manuscript ID	PY-ART-03-2020-000457.R1
Article Type:	Paper
Date Submitted by the Author:	01-Jul-2020
Complete List of Authors:	Liu, Xinhao; University of Akron, Polymer Science Jain, Tanmay; University of Akron, Polymer Science Liu, Qianhui; University of Akron, Polymer Science Joy, Abraham; University of Akron, Polymer Science

SCHOLARONE™ Manuscripts

ARTICLE

Structural Insight into the Viscoelastic Behaviour of Elastomeric Polyesters: Effect of the Nature of Fatty Acid Side Chains and the Degree of Unsaturation

Xinhao Liu,[a] Tanmay Jain,[a] Qianhui Liu[a] and Abraham Joy[*a]

ABSTRACT: Degradable polymers derived from sustainable sources, such as vegetable oils, provide an eco-friendly alternative to petroleum-based polymers. Vegetable oils are composed of triglycerides which differ in their fatty acid chain length and the degree of unsaturation. However, vegetable oils can vary greatly in their composition depending on the type of oil and region of cultivation, and hence, polymers made from such oils can result in heterogeneous polymer properties. Therefore, herein we synthesized three polyesters with different pendant fatty acid groups (linoleic acid C18:2, oleic acid C18:1, and stearic acid C18:0) and evaluated the effect of the structural difference on the rheological and mechanical properties of these vegetable oil based polyesters. Increasing the degree of unsaturation of the fatty acid side chains decreased the glass transition temperature, zero-shear viscosity, tensile strength, elongation at-break, and the recovery efficiency of elastic energy (resilience) of its crosslinked elastomer. We hypothesize that the cis double bonds introduce 'kinks' to the fatty acid side chains that impede the packing of the polymer chains and therefore, act as efficient 'internal diluents'. This is corroborated by an increase in the critical molecular weight for entanglement of the polymers with increasing number of cis double bonds in the side chains. Moreover, the presence of cis double bonds was associated with an increase in intermolecular friction and a decrease in the resilience. The structural insights derived from this study will be useful to design low modulus polymers and predict the processing and mechanical properties of polymers with fatty acid side chains.

Introduction

Due to environmental concerns, we are witnessing a concerted effort to replace petroleum-based polymers. A cornerstone of this effort is based on developing degradable polymers from naturally occurring and abundantly available vegetable oils .[1–7] Currently, most commercially available polymers such as polyethylene, polypropylene, and polyvinylchloride are derived from non-renewable resources and are non-degradable, leading to accumulation of plastic waste. Degradable polymers sourced from renewable sources such as vegetable oils offer a promising alternative to petroleum derived polymers.

Vegetable oils are composed of triglycerides (esterification product of glycerol and fatty acids) which differ primarily in their fatty acid chain length and the number of double bonds. The presence of double bonds allows the direct polymerization of triglycerides by using cationic polymerization.[1,8] Another strategy is to make monomers from vegetable oils by modifying the double bonds or the ester group. These monomers can undergo radical polymerization[4,9–11] or polycondensation to make polyesters[12,13], polyamides[14], or polyurethanes.[15–17] Such polymers are then used as thermoplastics[18], thermosets[8,19], and adhesives[20] due to their low cost and facile functionalization.

However, one of the major limitations of vegetable oil sourced polymers is the heterogeneity and variability of vegetable oil composition. For example, the majority of fatty acids in soybean oil triglycerides consist of linoleic acid C18:2 (53.3%), oleic acid C18:1 (23.4%), palmitic acid C16:0 (11%), linolenic acid C18:3 (7.8%), and stearic acid C18:0 (4%). Note that the nomenclature C18:2 refers to the number of carbons in the fatty acid (C18) and the degree of unsaturation (2). On the other hand, the fatty acid composition of corn oil triglycerides is linoleic acid C18:2 (59.6%), oleic acid C18:1 (25.4%), stearic acid C18:0(2%), linolenic acid C18:3 (1.2%), and palmitic acid C16:0 (10.9%).[1] Moreover, the fatty acid composition of the same oil may change based on the sourced region, batch, etc. This variability in the composition of fatty acids adversely affects the polymer processing and physicochemical properties. The polymer can vary from ductile to relatively brittle based on the type of the precursor vegetable oil.[19]

Therefore, it is critical to systematically study the effect of fatty acid composition (cis/trans configuration, chain length and the degree of unsaturation) on the resulting polymer properties. Longer chains of saturated fatty acids result in a semi-crystalline polymer due to the packing of the fatty acid side chains.[21] The cis configuration of unsaturated side chains has been shown to impede the packing of polymer chains which

[a]Department of Polymer Science, The University of Akron, Akron, OH 44325, USA
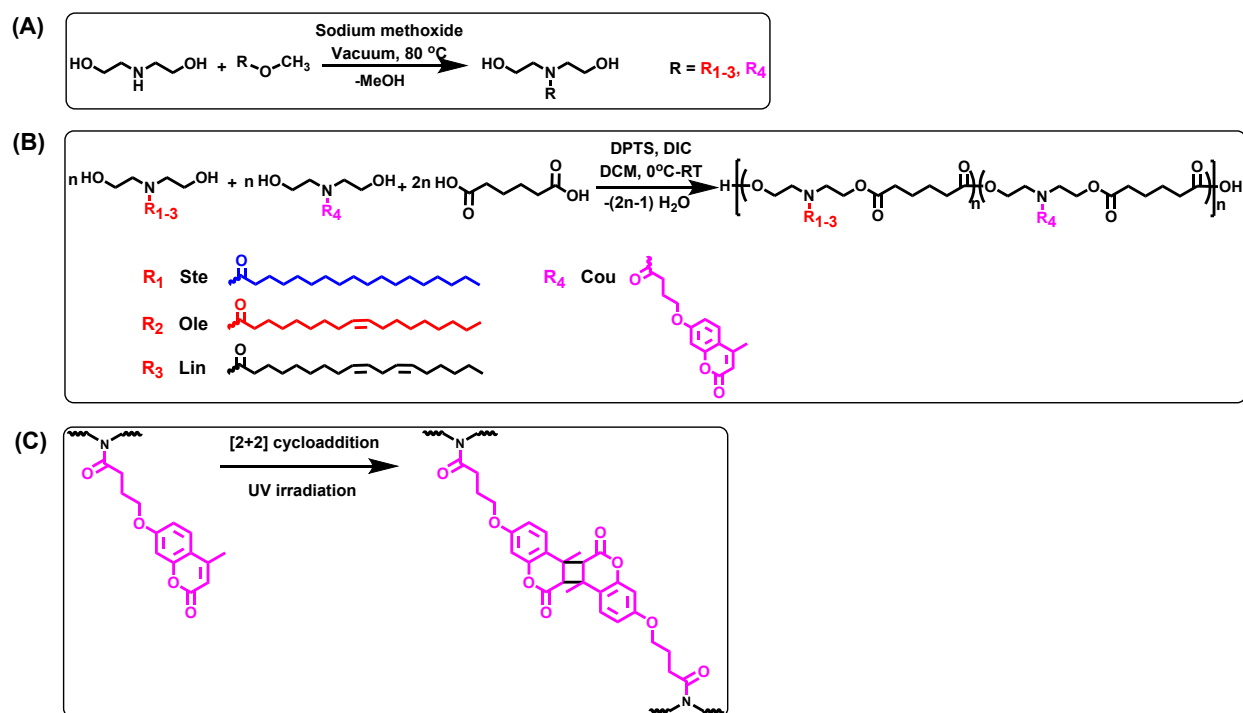
Scheme 1. Synthetic scheme for (A) the synthesis of diethanolamine derived monomers, (B) the synthesis of three polyesters (**p(Ste)**, **p(Ole)**, **p(Lin)**) with different pendant fatty acid groups, and (C) crosslinking of polymer chains by [2+2] cycloaddition reaction of coumarin.

disrupts crystallization and sacrifices mechanical properties of the polymer while the trans configuration allows for chain packing.[22,23] Although the effect of cis/trans configuration and chain length has been examined, to the best of our knowledge, the effect of the degree of unsaturation in fatty acid side chains on polymer properties has not been systematically examined. This limits our understanding of the intriguing physical properties of vegetable oil-based polymers, such as the observed high resilience of polyacrylates based on soybean oil.[11]

Herein, we synthesized and characterized polyesters with pendant fatty acid chains that vary only in their degree of unsaturation (Scheme 1). The fatty acid chains are the three most abundant and commonly present fatty acids in vegetable oils. Specifically, linoleic acid (C18:2), oleic acid (C18:1), and stearic acid (C18:0) were selected. These have the same chain length (C18) but different number of cis double bonds (2, 1, 0, respectively). The polyesters also contain a crosslinking coumarin group, which crosslinks through [2+2]-cycloaddition under UV irradiation ($\lambda > 310$ nm), to form elastomers for mechanical testing. The synthesis of the polyesters was confirmed using ^{1}H nuclear magnetic resonance (^{1}H NMR) and characterized by gel permeation chromatography (GPC), differential scanning calorimetry (DSC), rheology, and dynamic mechanical analysis (DMA) testing. We observed that the higher degree of unsaturation of fatty acid enhances the 'internal diluent' effect of alkyl side chains, reduces the zero-shear viscosity and glass transition temperature of polymers, and impedes polymer chain entanglements. Furthermore, the presence of double bonds decreases the ultimate tensile strength, elongation-at-break, and reduces the resilience of the

polymer networks due to the higher intermolecular friction and lack of entanglements. The structural insights derived from this study will assist in designing and predicting the processing and mechanical properties of vegetable oil-based polymers.

Experimental section

Materials.

All chemicals were used as received unless otherwise indicated. Potassium carbonate (99%), diethanolamine (99%), sodium methoxide (98%) were purchased from Alfa Aesar. 7-Hydroxy-4-Methylcoumarin (97%), adipic acid (99%) were purchased from Acros Organics. Methyl 4-Bromobutyrate (98.6%), 18-crown-6 (99%), lithium bromide (anhydrous, 99%), sodium formate (100%), 4-Dimethylaminopyridine (99.9%), *N,N′*-Diisopropylcarbodiimide (99.5%) (DIC) were purchased from Chem Impex. Sodium sulfate was purchased from VWR. Thionyl chloride (98%), *p*-Toluenesulfonic acid were purchased from TCI America. Linoleic acid (98%) was purchased from Combi-Blocks. Oleic acid (90%) was purchased from Sigma-Aldrich. 4-(Dimethylamino) pyridinium 4-toluene sulfonate (DPTS) was prepared according to literature methods.[24] Reagent grade dichloromethane (DCM) was purchased from Thermo Fisher Scientific and dried by distilling over anhydrous calcium hydride. Reagent grade dimethylformamide (DMF) was purchase from Thermo Fisher Scientific and dried by distilling over anhydrous calcium hydride. Reagent grade ethyl acetate (EtOAc), methanol (MeOH), hexane (Hex) were used as received from Thermo Fisher Scientific. Dry methanol was purchased from EMD Millipore. Silica gel (40-63 µm, 230 × 400 mesh) for column

chromatography was purchased from Sorbent Technologies, Inc. Chloroform-D (D, 99.85%) was purchased from Cambridge Isotope Lab. *N,N-bis(2-hydroxyethyl)-4-((4-methyl-2-oxo-2H-chromen-7-yl)oxy)butanamide (Cou)* was synthesized according to a literature method.[25]

Synthesis of fatty acid diol monomers.

General Procedure.[26] 1 equiv. fatty acid was added into a round-bottom flask equipped with a magnetic stir bar. The flask was subjected to -10 °C methanol/ice bath. The solution was vigorously stirred and followed by the dropwise addition of 1.5 equiv. thionyl chloride with addition funnel in 30 minutes. Then 8 equiv. methanol was added drop by drop. The reaction mixture was kept at room temperature for 12h. After reaction completion, the excess acid was neutralized using saturated sodium carbonate solution and extracted with DCM. The combined organic solution was washed with brine, dried with anhydrous sodium sulfate and concentrated to yield the corresponding crude fatty acid methyl ester. Methyl stearate was prepared from crude methyl oleate according to a published protocol.[27] The fatty acid methyl ester was then mixed with 2 equiv. diethanolamine, 0.1 equiv. sodium methoxide and a magnetic stir bar. The mixture was magnetically stirred at 80 °C for 3h under reduced pressure. The crude product was purified via column chromatography (10:90 MeOH:DCM).

(9Z,12Z)-N,N-bis(2-hydroxyethyl)octadeca-9,12-dienamide (Lin). R_f = 0.67, yellow viscous liquid. ^{1}H NMR (CHLOROFORM-d, 300MHz): δ = 5.19 - 5.53 (m, 4 H), 3.68 - 3.96 (m, 4 H), 3.34 - 3.66 (m, 6 H), 2.76 (t, J=6.0 Hz, 2 H), 2.25 - 2.55 (m, 2 H), 2.04 (q, J=6.5 Hz, 4 H), 1.54 - 1.72 (m, 2 H), 1.14 - 1.48 (m, 14 H), 0.71 - 1.10 ppm (m, 2 H).

N,N-bis(2-hydroxyethyl)oleamide (Ole). R_f = 0.67, pale yellow viscous liquid. ^{1}H NMR (CHLOROFORM-d, 300MHz): δ = 5.33 (s, 2 H), 3.80 (dt, J=18.6, 4.9 Hz, 4 H), 3.38 - 3.71 (m, 6 H), 2.26 - 2.50 (m, 2 H), 2.00 (d, J=5.6 Hz, 4 H), 1.54 - 1.73 (m, 2 H), 1.26 (s, 10 H), 1.30 (s, 11 H), 0.68 - 1.02 (m, 3 H).

N,N-bis(hydroxyethyl)stearamide (Ste). R_f = 0.68, white powder. ^{1}H NMR (CHLOROFORM-d, 300MHz): δ = 3.71 - 3.94 (m, 4 H), 3.53 (dt, J=18.2, 5.1 Hz, 4 H), 2.55 (br. s., 1 H), 2.19 - 2.48 (m, 3 H), 1.63 (br. s., 2 H), 1.16 - 1.43 (m, 30 H), 0.82 - 0.96 ppm (m, 3 H).

Synthesis of Polyester.

General Polyesterfication Procedure.[26,28] In a typical experiment, **Ste** (592.2 mg, 1.59 mmol, 0.5 equiv), **Cou** (557.8 mg, 1.59 mmol, 0.5 equiv), adipic acid (466.1 mg, 3.18 mmol, 1 equiv), and DPTS (375.5 mg, 1.27 mmol, 0.4 equiv) were added to a round bottom flask with a magnetic stir bar. The flask was sealed and purged with nitrogen for 15 mins. Dry DCM (6 mL) was then added under magnetic stirring. This mixture was cooled to 0 °C and DIC (1605.2 mg, 12.72 mmol, 4 equiv) was then added dropwise by syringe. The reaction was allowed to come to room temperature and stirred for 48h. The diisopropyl urea byproduct was filtered off. The filtrate was then concentrated under reduced pressure, purified via precipitation

into cold methanol, and dried in vacuum to give the final product.

Molecular characterization.

All NMR spectra were recorded on a Varian Mercury 300 MHz spectrometer. Most of size exclusion chromatography (SEC) analyses were performed on a TOSOH EcoSec HLC-8320 GPC equipped with the refractive index detector (RI) and the ultraviolet (UV) detector unless otherwise specified. Separation occurred over two PSS Gram Analytical SEC columns in series using 25 mM lithium bromide in DMF as eluent at a flow rate of 0.8 mL/min. Weight average molecular weight (M_w) and polydispersity ($Đ$) of polyesters samples were determined relative to polystyrene standards using RI signal. For the absolute molecular weight measurements, the TOSOH Ecosec HLC-8320 GPC equipped with a refractive index detector and a multiangle laser light scattering (miniDAWN, Wyatt) was used at 30 °C. 0.1 M lithium bromide in DMF was used as the eluent at a flow rate of 0.5 mL/min. Different concentrations of polymer in DMF (0.1M LiBr as the additive) were injected into Waters 2410 refractive index detector (temperature stabilized at 30 °C) for the dn/dc calculation.

Thermal Analysis.

Glass transition temperatures (T_g) and melting temperature (T_m) of the polyesters were determined using a TA Q2000 differential scanning calorimeter (DSC) with liquid nitrogen cooling unit. The samples were placed in hermetic pans and heated from -50 to 50 °C, cooled down to -50 °C, and heated back to 50 °C at a rate of 10 °C /min under nitrogen atmosphere. The T_g was determined from the midpoint of the inflection curve of the second heating scan. The T_m was defined as the temperature at the melting peak apex.

Rheology.

All the rheology experiments were performed on an Advance Rheometric Expansion System (ARES) G2 (TA Instruments, New Castle, DE) with either parallel plates geometry (diameter R = 8 mm) or cone and plate fixture. For the cone and plate geometry, diameter R = 8 mm, and the cone has a truncation t = 0.057 mm and angle α = 0.0872.

Flow sweep test. The zero-shear viscosity (η_0) of polyester melts were determined from the Newtonian plateau using the parallel plates geometry. The sample was loaded on the bottom plate, heated up to 50 °C, compressed into a cylinder shape and held for 6 mins to remove any air bubbles. Then the sample chamber was cooled back to 25 °C and conditioned for another 6 mins to equilibrate. Flow sweep test was then carried out under 25 °C atmosphere environment with the constant gap (~0.5 mm). The viscosity was recorded at a steady state shear sweep rate from 0.001 to 10 s^{-1}. Before the acquisition of each data point, the sample was allowed to equilibrate for 240 seconds.

Small-amplitude oscillatory shear (SAOS). For uncured polyester melt, the measurement was conducted with cone and plate geometry. The sample loading procedure was the same as
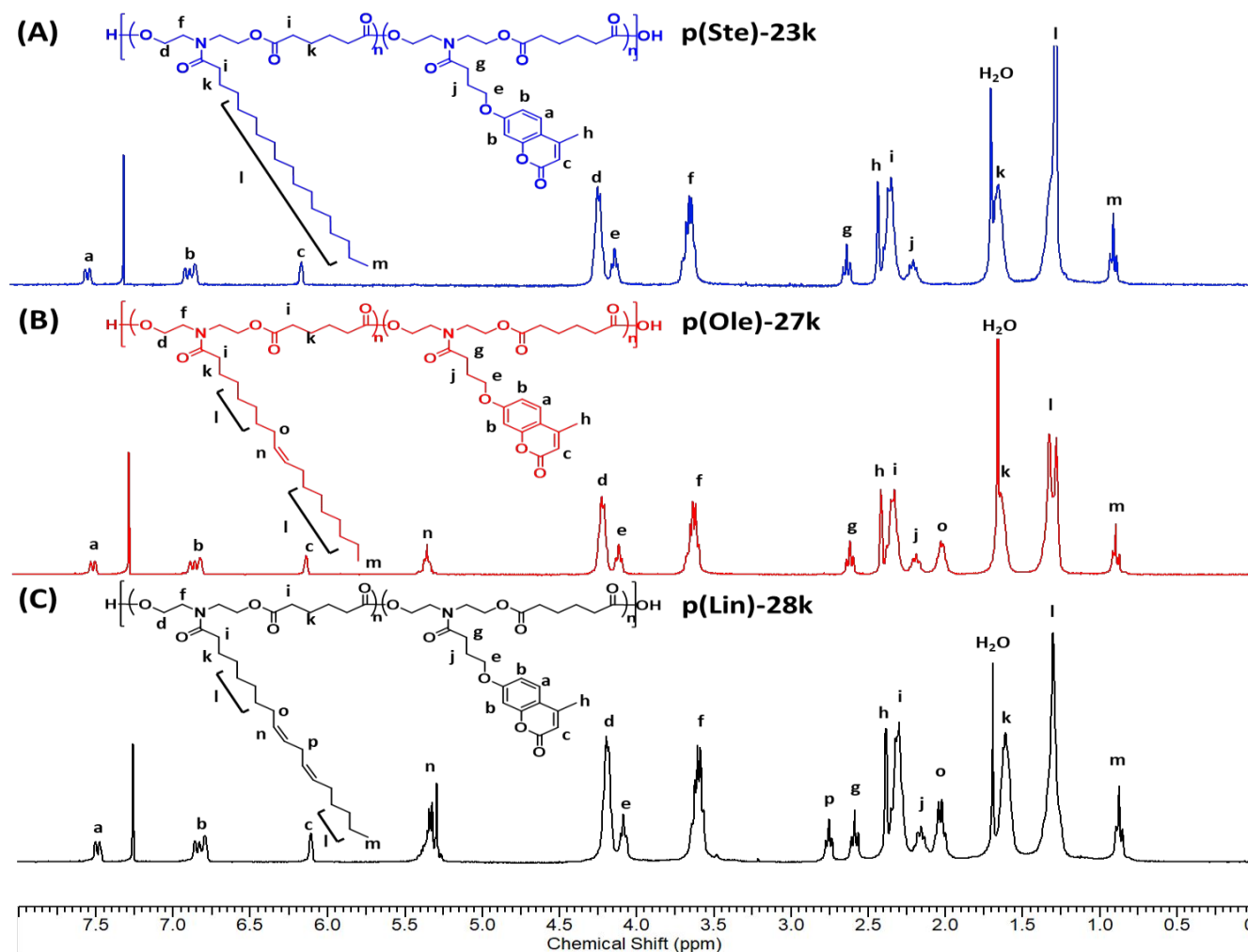
Figure 1. ^{1}H NMR (CDCl$_3$) spectra of (A) **p(Ste)-23k**, (B) **p(Ole)-27k**, and (C) **p(Lin)-28k**.

that for the flow sweep test. A strain sweep was performed prior to a frequency sweep to determine the linear viscoelastic region (LVE) for each polymer. The frequency sweeps were carried out at strain% within the LVE. The dynamic responses at different temperatures were recorded every 5 points per decade with a frequency range of 0.1-100 rad/s. Master curves were constructed by calculating shift factors using the WLF equation and shifting the data along the frequency axis to a reference temperature (T_{ref}) of 25 °C for all the samples. For the crosslinked polyesters, the strain sweep was conducted using parallel plates geometry rather than the cone plate fixture to ensure good contact between the sample and the plate. The gap was maintained at 1 mm. The UV crosslinking was performed outside the rheometer using an Omnicure S1500 (23 W/cm2 (source), λ = 320-500 nm). The distance between the top of the sample and light source was 5 cm. Prior to each experiment, the material was allowed to relax and reach 0 N (±0.02 N) normal force.

Mechanical Properties.

Tensile tests and cyclic tensile tests were carried on TA Q800 DMA in tensile mode at 25 °C. All the polyesters were frozen into a solid with liquid nitrogen and transferred into a mold (20

× 5 × 1 mm). Both sides of the mold were covered with polytetrafluoroethylene sheets. The sandwich was compressed at 50 °C for 1 h under vacuum to remove any bubbles and residual stress. The material was subsequently cooled down by liquid nitrogen to keep the shape during removal of the PTFE sheets. The materials were exposed to UV light (Omnicure S1500 23 W/cm^2 (at source), λ = 320-500 nm, 5 cm distance) for 360s, flipped over, and exposed for another 360s. For tensile tests, the specimen was subjected to 5% strain/minute elongation until the material failed at 25 °C. Cyclic tensile tests were conducted on the same instrument. In the first cycle, the sample was elongated to a 25% strain with a rate of 5% strain/min. Once the specimen reached 25% strain, the crosshead direction was reversed, and the sample strain was decreased at 1% strain/minute till stress was released to zero. The crosshead was immediately reversed to carry out the second cycle. The cyclic deformation was repeated 5 times.

Results and discussion

Synthesis of Monomers and Polymers.

Three fatty acids, linoleic acid, oleic acid, and stearic acid were selected for the synthesis of the polymers described herein, due to their varying degree of unsaturation, abundance in vegetable oils, and same chain length. The fatty acids were converted to corresponding methyl esters of the fatty acids and subsequently converted to diol monomers through transamidation with diethanolamine (Scheme 1).[26] Figure S1 shows the ^{1}H NMR spectra of the stearic acid based monomer **Ste**, oleic acid based monomer **Ole**, linoleic acid based monomer **Lin**, and the coumarin based monomer **Cou**.

The configurations of double bonds in **Lin** and **Ole** are determined by J coupling constants of vinylic hydrogens in ^{1}H NMR (Figure S2). For cis isomer, the J coupling constant is in the range of 6-14 Hz whereas the trans isomer has a J coupling constant between 11 to 18 Hz.[29] The J coupling constant of **Ole** (J = 5.56 Hz) and **Lin** (J = 6.15 Hz) indicates both **Ole** and **Lin** monomers are cis isomers, as is commonly observed in natural vegetable oils.

The polyesters were synthesized by carbodiimide mediated polyesterifaction of diols (**Cou**, **Ste**, **Ole**, **Lin**) and a diacid (adipic acid).[26,30] All polyesters contain 25% (mol %) of the fatty acid diol, 25% (mol %) of **Cou**, and 50% (mol %) of adipic acid. The monomer, **Cou**, was introduced to enable UV light assisted crosslinking to form elastomers. Coumarin and its derivatives undergo a [2+2] cycloaddition with UV light (λ > 310 nm) exposure. (Scheme 1)[13,20,31] The characteristic peaks for aromatic protons at 6.0-7.5 ppm in Figure 1 and Figure S1D indicates the presence of coumarin units.

The polymer nomenclature used here describes the fatty acid diol species and the weight average molecular weight (M_w) of the polyesters. For example, **p(Ste)-23k** refers to a statistical copolymer of 25% **Ste**, 25% **Cou**, and 50% adipic acid with relative weight average molecular weight (M_w) about 23 kDa. The representative ^{1}H NMR spectra of **p(Ste)-23k**, **p(Ole)-27k**, and **p(Lin)-28k** are presented in Figure 1 and peaks are assigned.

The composition of these synthesized polyesters was verified based on the ratio of the integration of peaks corresponding to the characteristic peaks of the monomers. For example, the ratio of integration areas of aromatic hydrogen (6.71 ppm) and methyl group at the end of fatty acid (0.87 ppm) in **p(Ste)-23k** (Figure 1A) was 1.91:3.00. The corresponding integration ratio between **Cou** (Figure S1D) and **Ste** (Figure S1A) was 1.97:3.00 using the methylene (4H, 3.75-4.00 ppm) adjacent to the hydroxyl group in each monomer as the reference. The calculated diol monomer ratio **Cou:Ste** in **p(Ste)-23k** was determined to be 47.1:52.9. Similarly, the ratio of **p(Ole)-27k** and **p(Lin)-28k** was determined to be 49.3:50.7 and 48.0:52.0, respectively. The molar ratio of **Cou** to fatty acid derived monomer calculated from ^{1}H-NMR is close to the feed ratio. Therefore, all synthesized polyesters can be assumed to have similar compositions with varying pendant fatty acid chain unsaturation. Note that to synthesize different M_w polyesters, the diol/diacid feed ratio was varied slightly. However, the **Cou** to fatty acid derived diol monomer feed ratio was kept constant (50:50).

Table 1 summarizes the physical and thermal properties of all the polyesters studied in this paper with M_w from 20 kDa to

66 kDa and polydispersity (Đ) of 1.5-2.25. Notice in Table 1 and Figure S6 that the T_g and T_m of **p(Ste)** do not change appreciably with increasing M_w. Moreover, T_g decreases with increasing number of cis-double bonds in the pendant fatty acid chains. The presence of cis double bonds introduces molecular kinks and inhibits the close packing of long alkyl side chains.[22] Consequently these loosely packed side chains serve as 'internal diluents' and contribute to the higher mobility of polymer chains resulting in lower T_g.[32–34] The melting peak of **p(Ste)-23k** (Figure S6) arises from the close packing of the long saturated alkyl chain (Scheme 2). Similar results are reported for stearic acid starch esters, and poly(styrene-*b*-(lauric acid-*co*-stearic acid)-*b*-styrene.[11,22]

In addition to the relative M_w measured by GPC using polystyrene as standards, the absolute M_w of three different polymers (relative M_w ~ 31±1 kDa) were determined as 25±1 kDa (Figure S5 and Table S1). The absolute M_w trend among three polymers is similar to the relative M_w trend which ensures the validity of the following conclusions drawing from property comparison at similar relative M_w.

Table 1. Physical properties of **p(Ste)**, **p(Ole)**, and **p(Lin)** at different molecular weights.

Polyester	M_n[a] (kDa)	M_w[a] (kDa)	Đ[a]	T_g[b] (°C)	T_m (°C)
p(Ste)-23k	15.8	23.5	1.48	-0.3	17.6
p(Ste)-37k	16.5	37.1	2.24	-0.3	16.3
p(Ste)-43k	22.6	43.7	1.94	-0.2	16.4
p(Ste)-47k	23.2	47.7	2.05	-0.1	16.2
p(Ste)-51k	23.5	51.5	2.19	0.1	16.2
p(Ste)-56k	27.4	56.6	1.95	-0.3	16.0
p(Ste)-66k	32.2	66.0	2.05	0.1	16.4
p(Ole)-20k	13.7	20.1	1.47	[c]	[c]
p(Ole)-27k	14.3	26.8	1.87	-20.4	N[d]
p(Ole)-33k	17.2	33.9	1.97	[c]	[c]
p(Ole)-43k	27.0	43.8	1.62	[c]	[c]
p(Ole)-50k	23.7	50.6	2.13	[c]	[c]
p(Lin)-20k	12.7	20.5	1.61	[c]	[c]
p(Lin)-28k	15.2	28.3	1.86	-24.7	N[d]
p(Lin)-36k	22.6	36.4	1.61	[c]	[c]
p(Lin)-42k	22.1	42.4	1.92	[c]	[c]
p(Lin)-47k	23.4	47.5	2.02	[c]	[c]
p(Lin)-53k	23.5	53.1	2.25	[c]	[c]

[a]Determined by GPC equipped with RI detector using DMF (with 25mM LiBr) as the eluent and PS as the standard.
[b]Glass transition temperature (T_g) and melting temperature (T_m) are determined by DSC.
[c]DSC experiment was not conducted as T_g does not vary significantly with M_w.
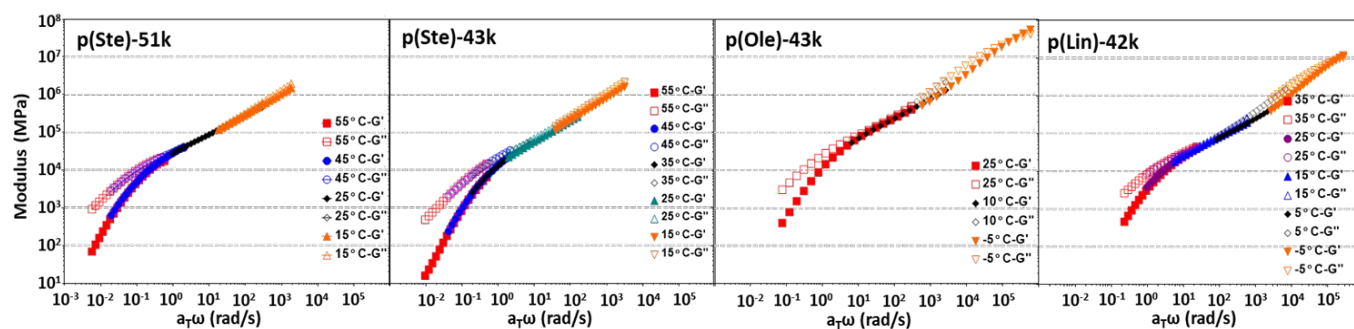[d]No melting peak was observed.

Figure 2. Comparison of the dynamic responses of the investigated **p(Ste)-51k**, **p(Ste)-43k**, **p(Ole)-43k,** and **p(Lin)-42k** at the reference temperature (25 °C).
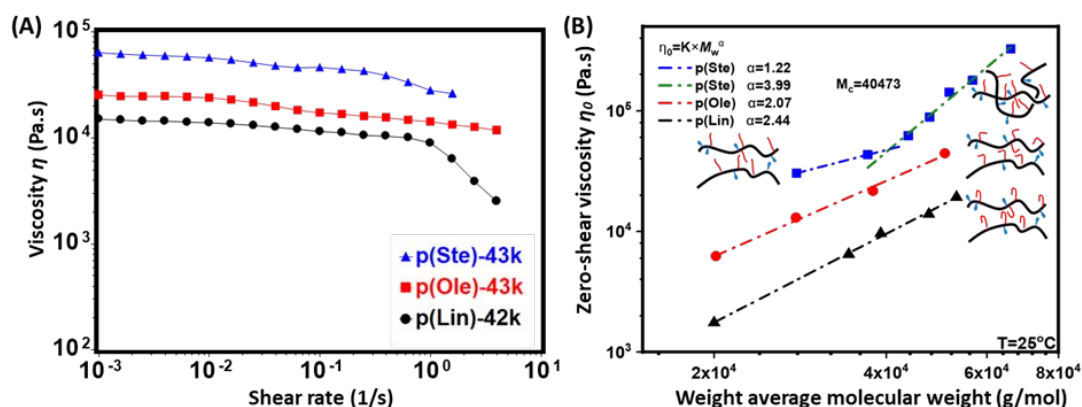

Figure 3. (A) Viscosity versus shear rate at 25 °C, η_0 is determined from the viscosity plateau. The solid curves are plotted by connecting experimental data points. (B) η_0 versus M_w at 25 °C. The dotted line in Figure 3B is obtained from linear fitting of experimental data (solid symbols) with $R^2 > 0.99$. The crossover between two lines of **p(Ste)** indicates the critical molecular weight for entanglement (M_c).

Rheology.

In Figure 2, we have compared the dynamic behaviours of three different polyesters. All polyesters are compared at similar M_w (~43 kDa) and **p(Ste)** at 51 kDa is also represented. The data collected at different temperatures was superimposed using time-temperature superposition (TTS) principle at the reference temperature of 25 °C. Generally, for polymer melts with molecular weight lower than the entanglement molecular weight ($M_w < M_e$), it is expected that predominantly viscous behaviour (G' < G'') will be observed in the measured frequency region. However, for $M_w > M_e$, a plateau region with G' > G'' emerges which is referred to as the entanglement plateau.[35,36] The validity of the TTS plot was verified by Van Gurp-Palmen
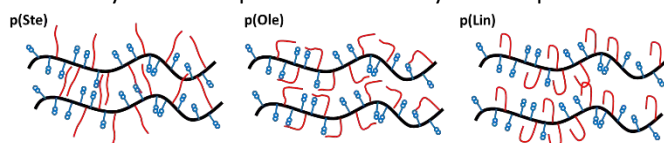
Scheme 2. Schematic representation of three polyesters (**p(Ste)**, **p(Ole)**, and **p(Lin)**) at similar M_w (< M_c). The blue, red and black solid lines represent the coumarin side group, fatty acid side chains, and the polyester backbone, respectively. The sharp kink in the side chain represents the cis double bond.

method by plotting the phase angle as a function of complex modulus (|G*|) (Figure S7). The Van Gurp-Palmen plots were smooth continuous curves for all the polyesters which validates the TTS plots. The minima in the Van Gurp-Palmen plot corresponds to the relaxation mechanisms of the polymer chain subunits. For example, the presence of two minima in the Van Gurp-Palmen plot corresponds to side chain relaxation and polymer chain relaxation.[37,38] However, in our case, only one minimum was observed for each curve which indicates a single relaxation mechanism for each polyester, which is polymer chain relaxation.[39–41] In Figure 2, G'' remains above G' for **p(Ste)-43k, p(Ole)-43k**, and **p(Lin)-42k** and G' overtakes G'' for **p(Ste)-51k** in 10^{-1}-10^{-4} rad/s shear rate region. For clarity, the data is plotted as tan (delta) versus angular frequency to identify the crossover of G' and G'' for all four polymers (Figure S8). Tan (delta) is the ratio of G'' and G'.

A plot of zero shear viscosity, η_0, as a function of log M_w can be used to identify the critical molecular weight for entanglement (M_c).[42] Note that M_c should not be confused with the molecular weight between entanglements (M_e). A formerly used rule of thumb is $M_c \sim 2M_e$ but Fetters *et. al.* has shown that the ratio, M_c/M_e, varies with polymer chemical structure.[43] As observed in Figure 3B, the scaling factor (α) of log η_0 as a
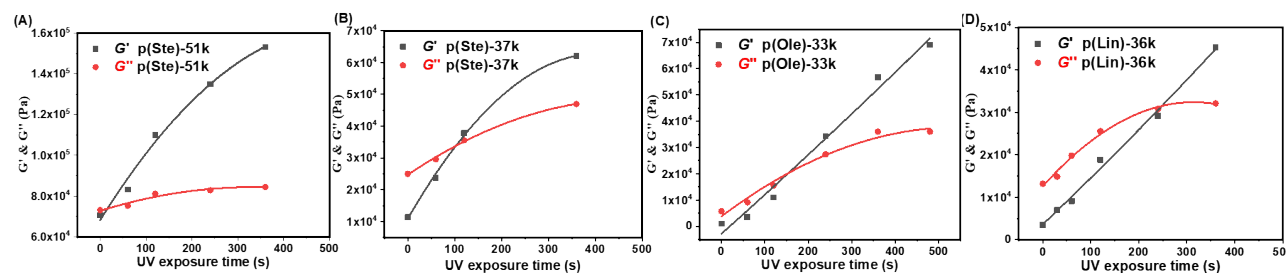
Figure 4. Effect of irradiation time on G' and G'' for (A) **p(Ste)-51k**, (B) **p(Ste)-37k**, (C) **p(Ole)-33k**, (D) **p(Lin)-36k** at 25 °C. The solid curves are polynomial fitting based on experimental data (solid symbols) with $R^2 > 0.975$.

function of log M_w is constant for **p(Lin)** and **p(Ole)** in the studied M_w range (22k to 53k), which is 2.44 and 2.07, respectively. Moreover, the absence of G'' and G' crossover in Figure 2 indicates the absence of polymer chain entanglements for **p(Lin)** and **p(Ole)** in the studied M_w range. In case of **p(Ste)**, the scaling factor is 1.22 (below M_c ~ 40.4 kDa) and 3.99 (above M_c). Most polymers such as poly(vinyl acetate), poly(vinyl chloride), poly(tetramethylene adipate), poly(ethylene terephthalate) etc. have a M_c of 4-15 kDa.[44] The absolute M_w of **p(Ste)** around M_c was determined to be 33k Da (Table S1 and Figure S5). In our case, the M_c is larger in case of **p(Ste)** than most common polymers and is not observed for **p(Ole)** and **p(Lin)**. Moreover, the M_e of **p(Ste)** was determined to be about 32.0 kg/mol based on equation $M_e = \rho RT/G_N^0$ (see SI for further discussion). The G_N^0 can be calculated based on the value of the complex modulus corresponding to the phase minima in the Van Gurp – Palmen plots of physically entangled polymers. We propose that the cis double bond 'fixes' the four carbons of the double bond in plane and inhibits chain packing leading to increased side chain flexibility, resulting in higher entanglement molecular weight for the polymer with the higher degree of unsaturation.

Mechanical Properties.

The polymer should be predominantly elastic to be amenable to mechanical testing. Therefore, coumarin groups were introduced which crosslink by a [2+2] cycloaddition reaction. The photo-crosslinking process was monitored by rheology tests by plotting the dynamic moduli as a function of UV

exposure time. As shown in Figure 4, UV irradiation (Omnicure S1500 23 W/cm² (at source), λ = 320-500 nm, 5 cm distance) induces crosslinking in all the polyesters, resulting in an increase of both G' and G''. Initially, the polymers are predominantly viscous (G''>G') and eventually transition to an elastomeric solid (G'> G'') with more UV exposure. Additional UV irradiation leads to further increase of the moduli beyond the transition point. Note that **p(Lin)** requires more crosslinking time to change to an elastomer than does **p(Ole)** and **p(Ste)**. This is due to the higher number of cis double bonds of **p(Lin)** which impede the packing of the polymer chains. Additionally, in case of **p(Ste)-51k**, G' overtakes G'' within 60 seconds under UV light exposure. This is due to the chain entanglements in **p(Ste-51k)**, which act as temporary crosslinks leading to significant increase in the elastic modulus.

All the tensile test samples were prepared by compression molding the polymers in a cast of size 20 mm × 5 mm × 1 mm, under vacuum. Since all polyesters formed an elastomer after 360 s UV exposure (Figure 4), all specimens were subjected to UV exposure for 360 s to cure the polyesters from the top and subsequently another 360 s from the bottom side. Since all the polymers have similar crosslinker composition and were irradiated for the same amount of time, the crosslinking density is expected to be similar. However we realize that the difference in chain unsaturation can result in differences in crosslinking density as a result of chain mobility difference and UV light (λ > 310 nm) absorptivity. (Swelling ratios of the polymers are provided in the supporting information, but due to lack of
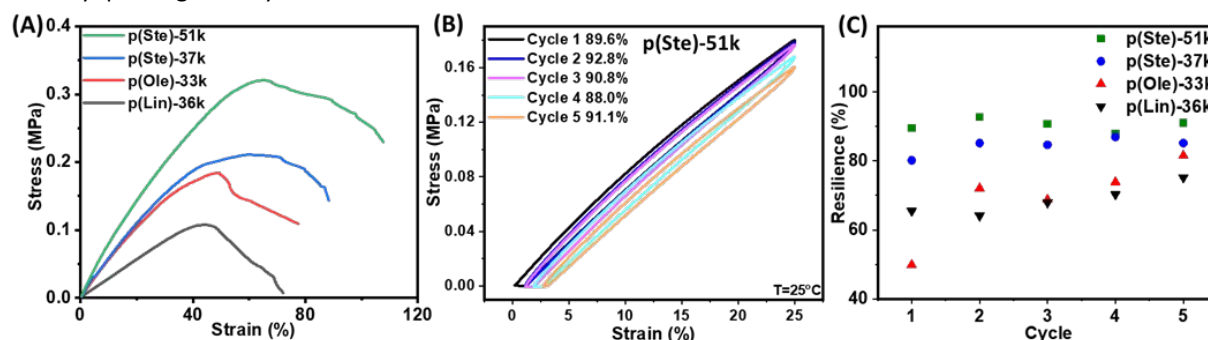

Figure 5. (A) Tensile tests of specimens from **p(Ste)-51k**, **p(Ste)-37k**, **p(Ole)-33k** and **p(Lin)-36k** at 25 °C. (B) Cyclic tensile test result of **p(Ste)-51k** at 25 °C. (C) Summarization of resilience obtained from cyclic tensile tests for **p(Ste)-51k**, **p(Ste)-37k**, **p(Ole)-33k** and **p(Lin)-36k** at 25 °C.

interaction parameters, the crosslinking density was not calculated.[45])

For all tensile tests, a TA Q800 DMA was used in the tensile mode. Tensile measurements were run at the speed of 5% strain/minute for all the samples. The results are summarized and plotted in Figure 5A and Figure S9. **p(Ste)-51k** network shows the highest mechanical strength (stiffness) compared to the other polyester networks. Compared to **p(Ste)-37k,** the **p(Ste)-51k** network has higher stiffness due to chain entanglements. Interestingly, **p(Ole)-33k** and **p(Ste)-37k** showed similar stiffness but different strain-at-break due to the cis double bond in the side chain of **p(Ole)-33k**. Similarly, **p(Lin)-36k** has the lowest stiffness and strain-at-break due to more cis double bonds in the side chains. The dependence of strain-at-break and stiffness on the number of cis double bonds in the polymer side chains provides a facile way to control the mechanical properties of vegetable oil derived elastomers.

Furthermore, the crosslinked polyesters were tested using cyclic tensile tests to determine their resilience (mechanical energy storage efficiency). The resilience behaviour depends on the crosslink density, uniformity of the polymer network, and intermolecular friction.[11,46] In our system, the difference in resilience between the polyester networks would arise mainly from the intermolecular friction. The cyclic tensile tests were performed at 25% strain which is within the elastic deformation regime of each polyester network. Figure 5B shows the representative curves for **pSte-51k**, and the cyclic test curves for the other polyester networks are presented in Figure S10. The resilience is obtained from the ratio of the area under the unloading curve and the loading curve. The resilience data is summarized and plotted in Figure 5C. We observed that **p(Ste)-37k** showed higher resilience behaviour than **p(Ole)-33k** and **p(Lin)-36k** showed the lowest resilience. In other words, less energy is dissipated for **p(Ste)-37k** due to less intermolecular friction in the network, and the trend in friction coefficient, ξ, is **p(Lin)**>**p(Ole)**>**p(Ste)** at similar M_w (36k). Moreover, according to the Rouse model, $\eta_0 = \xi N/18p$ (see SI for further discussion)[36], where ξ is the friction coefficient, N is the number of monomers in the polymer chain and p is the packing length. Therefore, for similar N, η_0 is directly proportional to ξ/p. Since η_0 is in the order of **p(Ste)**>**p(Ole)**>**p(Lin)** for similar N, **p(Ste)** can be expected to have highest ξ/p. As a result, we can derive that the packing length, p, is the lowest for **p(Ste)** and is the highest in the case of **p(Lin)**. The resilience of p(Ste)-51k reached 90% due to the combination of low intermolecular friction and polymer chain entanglements.

Conclusions

In summary, three polyesters (**p(Lin)**, **p(Ole)**, **p(Ste)**) functionalized with fatty acids chains of same length (linoleic acid C18:2, oleic acid C18:1, stearic acid C18:0) but which vary only in the number of cis double bonds, were synthesized and studied. The M_w ranged from 20 kDa to 66 kDa. The cis double bond introduces kinks in the fatty acid chains, impedes the packing of side chains and polymer chains. This leads to a decrease of T_g, η_0 and lack of polymer chain entanglement in

the studied M_w range for **p(Lin)** and **p(Ole)** when compared with **p(Ste)**, the polyester with saturated fatty acid chains. Moreover, intermolecular friction increases with increasing number of cis double bonds on each fatty acid side chain which is corroborated by the resilience behaviours of polyesters networks. Furthermore, the entanglement itself contributes to resilience by functioned as physical crosslinking and results in the high resilience of **p(Ste)-51k**. In all, the results show a correlation between the number of cis double bonds in the polymer side chains and the polymer dynamics and mechanical properties. These results and insight drawn from this study will contribute to the design of low modulus polymers, especially polymers with fatty acid side chains derived from vegetable oils.

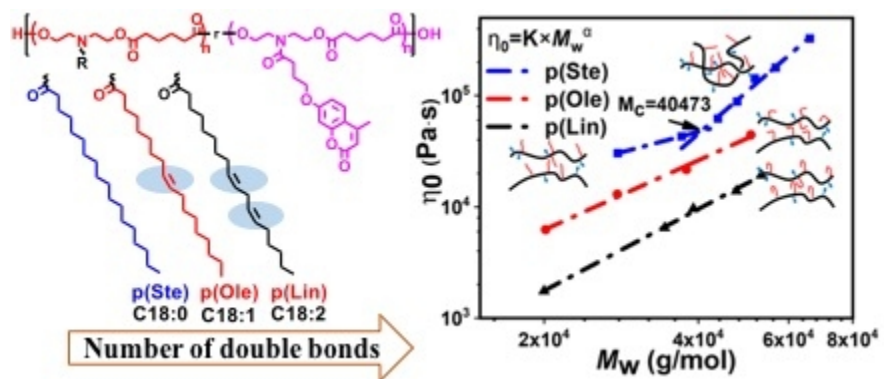## Conflicts of interest

There are no conflicts to declare.

Acknowledgements

References

1   Y. Xia and R. C. Larock, *Green Chem.*, 2010, **12**, 1893.
2   Z. Liu, Y. Xu, L. Cao, C. Bao, H. Sun, L. Wang, K. Dai and L. Zhu, *Soft Matter*, 2012, **8**, 5888.
3   G. Lligadas, J. C. Ronda, M. Galià and V. Cádiz, *Mater. Today*, 2013, **16**, 337–343.
4   S. Wang, S. Vajjala Kesava, E. D. Gomez and M. L. Robertson, *Macromolecules*, 2013, **46**, 7202–7212.
5   E. Kolanthai, K. Sarkar, S. R. K. Meka, G. Madras and K. Chatterjee, *ACS Sustain. Chem. Eng.*, 2015, **3**, 880–891.
6   L. Song, Z. Wang, M. E. Lamm, L. Yuan and C. Tang, *Macromolecules*, 2017, **50**, 7475–7483.
7   A. Nicolau, R. M. Mariath, E. A. Martini, D. dos Santos Martini and D. Samios, *Mater. Sci. Eng. C*, 2010, **30**, 951–962.
8   R. C. LI, F.; HANSON, M. V.; LAROCK, *Polymer (Guildf).*, 2001, **24**, 1567–1579.
9   Z. Wang, L. Yuan, N. M. Trenor, L. Vlaminck, S. Billiet, A. Sarkar, F. E. Du Prez, M. Stefik and C. Tang, *Green Chem.*, 2015, **17**, 3806–3818.
10   T. Pakula, Y. Zhang, K. Matyjaszewski, H. il Lee, H. Boerner, S. Qin and G. C. Berry, *Polymer (Guildf).*, 2006, **47**, 7198–7206.
11   L. Yuan, Z. Wang, M. S. Ganewatta, M. A. Rahman, M. E. Lamm and C. Tang, *Soft Matter*, 2017, **13**, 1306–1313.
12   J. D. Hackenberg, N. D. Stebbins and K. E. Uhrich, *Macromol. Chem. Phys.*, 2017, **218**, 1–5.
13   S. R. Govindarajan, Y. Xu, J. P. Swanson, T. Jain, Y. Lu, J. W. Choi and A. Joy, *Macromolecules*, 2016, **49**, 2429–2437.
14   N. Kolb, M. Winkler, C. Syldatk and M. A. R. Meier, *Eur. Polym. J.*, 2014, **51**, 159–166.
15   S. D. Rajput, D. G. Hundiwale, P. P. Mahulikar and V. V.

Gite, *Prog. Org. Coatings*, 2014, **77**, 1360–1368.

16   H. L., K. X. and N. S.S., *Biomacromolecules*, 2009, **10**, 884–891.

17   G. Gultekin, C. Atalay-Oral, S. Erkal, F. Sahin, D. Karastova, S. B. Tantekin-Ersolmaz and F. S. Guner, *J. Mater. Sci. Mater. Med.*, 2009, **20**, 421–431.

18   L. Maisonneuve, T. Lebarbé, E. Grau and H. Cramail, *Polym. Chem.*, 2013, **4**, 5472.

19   F. Li and R. C. Larock, *J. Polym. Sci. Part B Polym. Phys.*, 2001, **39**, 60–77.

20   Y. Xu, Q. Liu, A. Narayanan, D. Jain, A. Dhinojwala and A. Joy, 2017, **1700506**, 1–6.

21   A. Vanmarcke, L. Leroy, G. Stoclet, L. Duchatel-Crépy, J. M. Lefebvre, N. Joly and V. Gaucher, *Carbohydr. Polym.*, 2017, **164**, 249–257.

22   A. Pipertzis, A. Hess, P. Weis, G. Papamokos, K. Koynov, S. Wu and G. Floudas, *ACS Macro Lett.*, 2018, **7**, 11–15.

23   S. Ito, A. Yamashita, H. Akiyama, H. Kihara and M. Yoshida, *Macromolecules*, 2018, **51**, 3243–3253.

24   J. S. Moore and S. I. Stupp, *Macromolecules*, 1990, **23**, 65–70.

25   Q. Liu, T. Jain, C. Peng, F. Peng, A. Narayanan and A. Joy, *Macromolecules*, , DOI:10.1021/acs.macromol.9b02558.

26   S. Gokhale, Y. Xu and A. Joy, *Biomacromolecules*, 2013, **14**, 2489–2493.

27   O. Arkad, H. Wiener and N. Garti, *J. Am. Oil Chem. Soc.*, 1987, **64**, 1529–1532.

28   Q. Liu, C. Wang, Y. Guo, C. Peng, A. Narayanan, S. Kaur, Y. Xu, R. A. Weiss and A. Joy, *Macromolecules*, 2018, **51**, 9294–9305.

29   M. Karplus, *J. Am. Chem. Soc.*, 1963, **85**, 2870–2871.

30   T. Jain, D. Saylor, C. Piard, Q. Liu, V. Patel, R. Kaushal, J. W. Choi, J. Fisher, I. Isayeva and A. Joy, *ACS Biomater. Sci. Eng.*, 2019, **5**, 846–858.

31   S. R. Trenor, A. R. Shultz, B. J. Love and T. E. Long, *Chem. Rev.*, 2004, **104**, 3059.

32   O. K. C. Tsui and H. F. Zhang, *Macromolecules*, 2001, **34**, 9139–9142.

33   A. Mpoukouvalas, W. Li, R. Graf, K. Koynov and K. Matyjaszewski, *ACS Macro Lett.*, 2013, **2**, 23–26.

34   T. Jain, W. Clay, Y.-M. Tseng, A. Vishwakarma, A. Narayanan, D. Ortiz, Q. Liu and A. Joy, *Polym. Chem.*, 2019, 5543–5554.

35   R. S. Porter and J. F. Johnson, *Chem. Rev.*, 1966, **66**, 1–27.

36   S.Q. Wang, *Nonlinear polymer rheology*, Wiley, Hoboken, NJ, 2018.

37   M. Hu, Y. Xia, G. B. McKenna, J. A. Kornfield and R. H. Grubbs, *Macromolecules*, 2011, **44**, 6935–6943.

38   S. Trinkle and C. Freidrich, *Rheol. Acta*, 2001, **40**, 322–328.

39   S. Trinkle, P. Walter and C. Friedrich, *Rheol. Acta*, 2002, **41**, 103–113.

40   Y. Lin, Y. Wang, J. Zheng, K. Yao, H. Tan, Y. Wang, T. Tang and D. Xu, *Macromolecules*, 2015, **48**, 7640–7648.

41   M. Ahmadi, S. Pioge, C. A. Fustin, J. F. Gohy and E. Van Ruymbeke, *Soft Matter*, 2017, **13**, 1063–1073.

42   J. M. Dealy, R. G. Larson, J. M. Dealy and R. G. Larson, *Structure and rheology of molten polymers: from structure to flow behavior and back again*, Carl Hanser Verlag GmbH Co KG, 2018.

43   L. J. Fetters, D. J. Lohse, D. Richter, T. A. Witten and A. Zirkel, *Macromolecules*, 1994, **27**, 4639–4647.

44   G. L. Wilkes, *J. Chem. Educ.*, 1981, **58**, 880.

45   R. S. H. Wong, M. Ashton and K. Dodou, *Pharmaceutics*, 2015, **7**, 305–319.

46   J. Cui, M. A. Lackey, A. E. Madkour, E. M. Saffer, D. M. Griffin, S. R. Bhatia, A. J. Crosby and G. N. Tew, *Biomacromolecules*, 2012, **13**, 584–588.

154x65mm (72 x 72 DPI)